Acta Crystallographica Section D
Biological Crystallography
ISSN 0907-4449

Alternate conformations observed in catalytic serine of *Bacillus subtilis* lipase determined at 1.3 Å resolution

Kosei Kawasaki,[a] Hidemasa Kondo,[a]* Mamoru Suzuki,[b] Satoru Ohgiya[a] and Sakae Tsuda[a]

[a]Structural Biology Group, Research Institute of Biological Resources, National Institute of Advanced Industrial Science and Technology (AIST), 2-17-2-1 Tsukisamu-Higashi, Toyohira, Sapporo 062-8517, Japan, and [b]Photon Factory, Institute of Materials Structure Science (IMSS), High Energy Accelerator Research Organization (KEK), 1-1 Oho, Tsukuba, Ibaraki-ken 305-0801, Japan

Correspondence e-mail: h.kondo@aist.go.jp

Received 28 February 2001
Accepted 18 April 2002

PDB Reference: lipase, 1isp, r1ispsf.

Bacillus subtilis extracellular lipase (BsL) has an exceptionally low molecular weight (19.4 kDa) for a member of the lipase family. A crystallographic study was performed on BsL in order to design and produce mutant BsL that will be more suitable for industrial uses based on analysis of the three-dimensional structure. Recently, the crystal structure of BsL has been determined at 1.5 Å resolution [van Pouderoyen *et al.* (2001). *J. Mol. Biol.* **309**, 215–226]. In the present study, a new crystal form of BsL which provides diffraction data to higher resolution was obtained and its structure was determined at 1.3 Å using the MAD method. It was found that the active-site residue Ser77 has alternate side-chain conformations . The O^{γ} atom of the first conformer forms a hydrogen bond to the N^{ε} atom of His155, a member of the catalytic triad. In contrast, the second conformer is constructed with a hydrogen bond to the side-chain atom of the adjacent His76. These two conformers presumably correspond to the active and inactive states, respectively. Similar alternate conformations in the catalytic serine residue have been observed in *Fusarium solani* cutinase determined at 1.0 Å resolution and *Penicillium purpurogenum* acetylxylan esterase at 0.9 Å resolution. In addition, a glycerol molecule, which was used as a cryoprotectant, is found to be located in the active site. On the basis of these results, a model for substrate binding in the reaction-intermediate state of BsL is proposed.

1. Introduction

Lipase (triacylglycerol lipase; EC 3.1.1.3) exists ubiquitously in various organisms; its function is to hydrolyze the ester bonds of long-chain triacylglycerols. Lipase is also involved in the catalytic processes of esterification, transesterification and enantioseparation of glycerols and organic acids (Jaeger *et al.*, 1994). Some of these catalytic activities are preserved even in organic solvent (*e.g.* hexane; Mustranta *et al.*, 1993). Lipase exhibits a vast divergence with regard to substrate specificity and the optimum conditions for enzymatic reaction such as temperature, pH and ionic strength. Hence, lipase is widely used for a variety of industrial processes and many devices have been developed to modify and improve its activity, including recent molecular-evolution techniques such as error-prone PCR and DNA shuffling. Lipase is generally secreted from cells to the medium and therefore it is easy to assay the activity for selection of the mutants. Together with these techniques, detailed understanding of the three-dimensional structure of lipase is indispensable to undertake the molecular design and production of modified versions of lipase.

Bacillus subtilis extracellular lipase (BsL), encoded by the *lipA* gene (Dartois *et al.*, 1992), has a molecular weight of 19.4 kDa, which is exceptionally low for a member of the bacterial lipase family; the range is generally 30–75 kDa. BsL is stable even under highly alkaline conditions (pH 12) and has optimal activity at pH 10; it is therefore regarded as an alkaliphilic lipase (Lesuisse *et al.*, 1993). The activities of ordinary lipases are known to be enhanced greatly in the presence of their substrate lipid micelle (Sarda & Desnuelle, 1958), implying that lipases act on their substrates at the lipid–water interface (so-called 'interfacial activation'). The enzymatic activity of BsL, however, does not depend on the formation of the substrate micelle, indicating that BsL possesses no interfacial activation, and takes place even at a low concentration of the substrate. Because of these unique characteristics, BsL is thought to be widely applicable to industrial uses and is a suitable target enzyme for close examination of three-dimensional structure.

The three-dimensional structures of lipase variants have been determined by X-ray crystallography (Derewenda, 1994). They share a common topology named the α/β-hydrolase fold (Ollis *et al.*, 1992) consisting of a six- to eight-stranded parallel β-sheet. The β-sheet is connected through α-helices, which are generally located surrounding the β-sheet. The active site of lipase is constructed in the C-terminal portion of the β-sheet and consists of Ser, His and Asp or Glu (the catalytic triad). In ordinary lipases, the active site is buried by a hydrophobic 'lid' consisting of one or two α-helices in the absence of micelle (Brzozowski *et al.*, 1991; Derewenda *et al.*, 1992). It should be noted that the α/β-hydrolase fold has not only been found in lipase variants but also in a wide variety of other hydrolytic enzymes including esterase and aminopeptidase. Despite high similarities in their three-dimensional structures, their amino-acid sequences show very little identity. Recently, the crystal structure of BsL was determined using crystals with space group $P2_12_12_1$ and unit-cell parameters $a = 39.64$, $b = 83.20$, $c = 95.75$ Å (van Pouderoyen *et al.*, 2001). This crystal structure at 1.5 Å resolution revealed that BsL forms a typical α/β-hydrolase fold consisting of a six-stranded parallel β-sheet surrounded by five α-helices. Here, we have performed independent BsL crystal growth and have obtained BsL crystals which have different unit-cell parameters ($a = 38.2$, $b = 58.5$, $c = 82.3$ Å) to those of van Pouderoyen and coworkers, despite belonging to the same space group. Our BsL crystals allowed us to obtain X-ray diffraction data to 1.3 Å resolution.

In the present paper, we describe the crystal structure determination of BsL at 1.3 Å resolution using the multi-wavelength anomalous diffraction (MAD) method. In this high-resolution structure, we observed two conformations at the active site, which presumably correspond to the active and inactive forms of the enzyme. Furthermore, we observed a glycerol molecule that is regarded as a reaction product. On the basis of the structural comparisons with cutinase from *Fusarium solani* (Longhi *et al.*, 1997) and acetylxylan esterase from *Penicillium purpurogenum* (Ghosh *et al.*, 2001), both of which exhibit a high degree of structural similarity with BsL despite having a very low degree of amino-acid sequence conservation, we propose a model for substrate binding in the reaction-intermediate state of BsL.

2. Methods and results

2.1. Protein preparation

The DNA fragment containing the *lipA* gene was amplified by PCR with chromosomal DNA prepared from *B. subtilis* 168 DSM402. Amplified DNA fragments were cloned into plasmid vector pWH1520 (BoBiTec, Germany). *B. megaterium* WH320 protoplast (MoBiTec) was transformed by the resultant plasmid (designated pWSL1) according to the protocol provided by the supplier. The transformant was cultured at 310 K with reciprocal shaking in LB medium (Sambrook *et al.*, 1989) supplemented with tetracycline (10 µg ml^{-1}). The culture supernatant was obtained by centrifugation after addition of 0.5%(*w*/*v*) D-xylose to induce the expression of BsL; solid ammonium sulfate was then added to 80% saturation and the pH was adjusted to 8.0 with ammonium hydroxide. After continuous stirring for 16 h at 277 K, precipitate was separated by centrifugation, dissolved in buffer *A* (20 m*M* sodium phosphate pH 6.8) and then dialyzed overnight against buffer *A*. The dialysate was applied to a MacroPrep High-S (Bio-Rad Laboratories) column equilibrated with buffer *A* and the adsorbed protein was eluted with a linear NaCl gradient (0.2–0.7 *M*). The lipase activity of each fraction was assayed with *p*-nitrophenyl butyrate as the substrate. Active fractions were pooled and desalted using a Sephadex-G50 (Amersham Pharmacia Biotech) column equilibrated with buffer *A*. The solution was applied to a Uno-S (Bio-Rad) column equilibrated with buffer *A* and the adsorbed protein was eluted with a linear NaCl gradient (0–0.5 *M*). Active fractions were pooled and desalted using Sephadex-G50 column equilibrated with buffer *B* (20 m*M* glycine–NaOH buffer pH 10.8). The resultant solution was applied to a Uno-Q (Bio-Rad) column equilibrated with buffer *B* and the adsorbed protein was eluted with a linear NaCl gradient (0–0.5 *M*). Active fractions were combined as the purified enzyme. Prior to crystallization, the purified BsL was rebuffered in 20 m*M* Tris–HCl pH 7.5 and concentrated to 15 mg ml^{-1} by ultrafiltration. The N-terminal amino-acid sequence was determined to be AEHNPVVMV, which was identical with that of BsL produced by *B. subtilis* 168 (Dartois *et al.*, 1992; Lesuisse *et al.*, 1993).

2.2. Crystallization and structure determination

We attempted initial screening of the crystallization conditions according to the sparse-matrix sampling method (Jancarik & Kim, 1991) using Crystal Screen (Hampton Research, CA, USA). The hanging-drop vapour-diffusion method (McPherson, 1990) was applied at 293 K for the crystallization. The droplet size was 6 µl, comprising the same volumes of BsL and reservoir solution. The initial conditions where crystals appeared were refined by varying the pH of the buffer and the concentration of the precipitant. The best

crystals of BsL were grown from 100 m*M* Tris–HCl buffer pH 8.7–8.8, 6–9%(*w*/*v*) polyethylene glycol 8000 and 17%(*v*/*v*) glycerol in about one week. They were prism-shaped crystals of approximately 0.5 × 0.5 × 1.0 mm in size.

Data from the native crystal were collected at 100 K on beamline 6A at the Photon Factory, KEK, Japan using an ADSC Quantum 4R CCD detector with 1.000 Å radiation and were processed with *DPS* (Rossmann & van Beek, 1999), *MOSFLM* (Powell, 1999) and the *CCP4* program suite (Collaborative Computational Project, Number 4, 1994). The crystal belongs to the orthorhombic space group $P2_12_12_1$, with unit-cell parameters a = 38.2, b = 58.5, c = 82.3 Å. Assuming one molecule in an asymmetric unit, V_M and the solvent content (Matthews, 1968) were calculated to be 2.5 Å^3 Da^{-1} and 50.6%, respectively. Diffraction intensities of the native crystal were collected to 1.3 Å resolution with an R_{merge} of 0.068 and a completeness of 96.5%.

MAD data were collected on beamline 18B at the Photon Factory equipped with a CCD detector and were processed in the same way as the native data. Intensity data at four wavelengths were collected to 1.85 Å at 100 K using a platinum-derivative crystal prepared by soaking the crystal in crystallization solution containing 5 m*M* $K_2Pt(NO_2)_4$ for 24 h. Table 1 summarizes the conditions and statistics of the data collections. The three platinum sites were determined and refined in order to calculate structure-factor phases using *SOLVE* (Terwilliger & Berendzen, 1999). The density map with initial phases was further improved using *RESOLVE* (Terwilliger, 2000). The data set of the native crystal was then input into *ARP*/*wARP* (Lamzin & Wilson, 1993; Perrakis *et al.*, 1997) and the resolution was expanded to 1.3 Å. Tracing the electron density and the model building for the BsL molecule was carried out automatically using *ARP*/*wARP*, giving a model containing 177 residues of 181 (His3–Thr179).

Table 1
Data-collection statistics of native and Pt-derivative crystals.

Values in parentheses are for the highest resolution shell.

Crystal	Native	5 m*M* $K_2Pt(NO_2)_4$, 24 h			
Beamline	PF BL6A	PF BL18B			
Wavelength (Å)	1.000	1.0718 (peak)	1.0721 (edge)	0.9800 (remote 1)	1.0800 (remote 2)
Resolution (Å)	1.3				
R_{merge}†	0.068 (0.315)	0.035 (0.148)	0.034 (0.142)	0.039 (0.133)	0.033 (0.134)
R_{ano}‡		0.053 (0.118)	0.039 (0.117)	0.042 (0.101)	0.028 (0.113)
Observed reflections	169453	50543	46572	56939	49119
Independent reflections	44447	15799	15214	16414	15599
Completeness (%)	96.5 (79.9)	96.5 (76.8)	93.0 (57.7)	99.9 (100.0)	95.2 (69.6)
Multiplicity	3.8 (3.1)	3.2 (1.9)	3.1 (1.6)	3.5 (3.3)	3.1 (1.7)
$\langle I/\sigma(I)\rangle$	6.5 (2.2)	15.9 (5.0)	16.4 (5.3)	11.7 (5.0)	16.7 (5.2)
R_{iso}§		0.310 (0.346)	0.308 (0.334)	0.326 (0.385)	0.317 (0.362)
Unit-cell parameters (Å)	a = 38.2, b = 58.5, c = 82.3	a = 38.1, b = 58.2, c = 82.9			

† $R_{merge} = \sum_j \sum_i |\langle I(h)\rangle - I(h)_j| / \sum_j \sum_i \langle I(h)\rangle$, where $\langle I(h)\rangle$ is the mean intensity of a set of equivalent reflections. ‡ $R_{ano} = \sum |I(+h) - I(-h)| / \sum [I(+h) + I(-h)]$. § $R_{iso} = \sum \big||F_{\lambda j}| - |F_{native}|\big| / \sum |F_{native}|$, where $F_{\lambda j}$ is the structure factor of derivative data at λ_j.

Table 2
Statistics for the refinement (using 44 447 unique reflections in the resolution range 20–1.3 Å).

Values in parentheses are for the highest resolution shell.

R factor†	0.192 (0.265)
Free *R* factor	0.232
Residues	179
Number of non-H atoms	
Protein‡	1369
Water	151
Glycerol	6
R.m.s bond length (Å)	0.029
R.m.s bond angle (°)	2.36

† *R* factor = $\sum \big||F_{obs}(h)| - |F_{calc}|\big| / \sum |F_{obs}(h)|$ where F_{obs} and F_{calc} are the observed and calculated structure factors, respectively. ‡ The final model includes alternate conformations of the side chains for Lys23, Asp34, Arg57, Glu65 and Ser77.

2.3. Structure refinement

A randomly chosen 3.0% of the X-ray diffraction data were used for calculation of the free *R* factor (Brünger, 1992). After several cycles of iteration of refinement with *CNS* (Brünger *et al.*, 1998) against the 20–1.3 Å intensity data and correction of the model using *O* (Jones *et al.*, 1991), water molecules were introduced into the model. Further refinement was carried out with *SHELX*97 (Sheldrick & Schneider, 1997). The *B* factors were treated as isotropic throughout the refinement. At this stage, side chains with alternate conformations were identified in several residues, such as Lys23, Asp34, Arg57, Glu65 and Ser77, all of which are located at the molecular surface. Occupancies of each alternate conformation were fixed to be equal throughout the refinement. After several cycles of refinement, electron density which presumably corresponds to a glycerol molecule was identified. This glycerol was also introduced into the BsL model. The final model has 1369 non-H atoms, corresponding to 179 BsL residues, 151 water molecules and six glycerol atoms, giving an *R* factor of 0.192 and a free *R* factor of 0.232. Two residues at both termini were not visible in the electron-density map and were not included in the current model. A summary of the refinement is listed in Table 2.

2.4. Overall structure

Fig. 1 shows a schematic model of BsL. Secondary-structure assignments were performed with *PROCHECK* (Laskowski *et al.*, 1993) using the criteria of Kabsch & Sander (1983). Eleven major secondary structures were clearly identified in BsL. They are six parallel β-sheet strands, β1 (3–12), β2 (35–42), β3 (71–77), β4 (97–103), β5 (123–130) and β6 (146–152), the principal elements of the globular structure, and five α-helices, α1 (16–28), α2 (48–66), α3 (78–89), α4 (157–161) and α5 (163–173), which appear to connect the β-strands and further flank

the β-sheet region. Several short helical segments are also identified, mainly in the loop regions.

2.5. Structure quality

The torsion angles of the main-chain atoms were analyzed using a Ramachandran plot (Ramakrishnan & Ramachandran, 1965) produced by *PROCHECK* (Laskowski *et al.*, 1993). Most residues fell into the most favoured and additional allowed regions. One residue fell into the disallowed region: Ser77, which is a member of the catalytic triad (Misset *et al.*, 1994). Ser77 connects β-strand β3 and α-helix α3. As a consequence of the unusual φ and ψ angles of Ser77, this residue forms an ε-conformation and constructs a sharp turn called a γ-turn. Unusual torsion angles around the catalytic serine residue are commonly found in many other α/β-hydrolase structures.

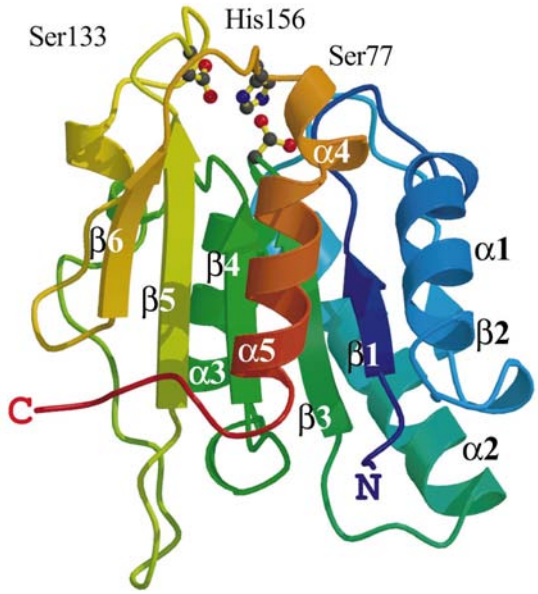

Figure 1
A schematic drawing of BsL produced with *MOLSCRIPT* (Kraulis, 1991) and *RASTER3D* (Merritt & Bacon, 1997). Secondary structures are labelled (β1–β6, α1–α5). The side chains of the catalytic triad (Ser77, Asp133 and His156) are represented in ball-and-stick. The N- and C-termini are denoted N and C, respectively.

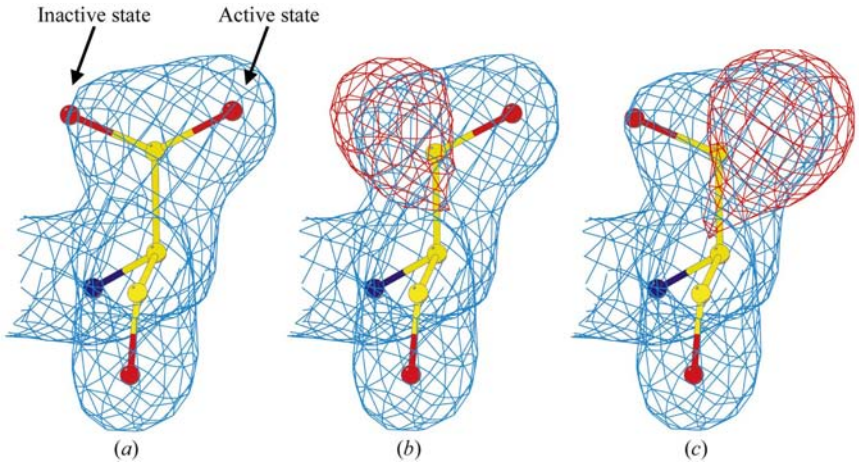

Figure 2
Alternate conformations of the O^{γ} atom of Ser77. σ_A-weighted (Read, 1986) $2F_o - F_c$ and $F_o - F_c$ maps are shown in blue and red, respectively. (*a*) The σ_A-weighted $2F_o - F_c$ map is calculated using two conformers in the side chain of Ser77. The O^{γ} atoms corresponding to the active and inactive states are labelled with arrows. (*b*) and (*c*) By omitting each conformer for Ser77, the difference electron density for the remainder appears in each $F_o - F_c$ map. The contour level for the σ_A-weighted $2F_o - F_c$ map is 2σ and that for the $F_o - F_c$ map is 2.5σ. This figure and the following figures were produced with *BOBSCRIPT* (Esnouf, 1997) and *RASTER3D*.

3. Discussion

3.1. Comparison with other structures and packing in the crystal lattice

The crystal structure of BsL has been reported at 1.5 Å resolution (van Pouderoyen *et al.*, 2001). The crystal used for the structure determination in this analysis contains two BsL molecules (*A* and *B*) in the asymmetric unit. Root-mean-square distances of C^{α} atoms between the present structure and van Pouderoyen's structure are estimated to be 0.29 Å for molecule *A* and 0.80 Å for molecule *B*, implying that the overall structure of the BsL molecule determined in the present study is almost identical to the previously reported structure. Large differences, however, appeared in molecule *B* in the following two regions: Ile12–Ala15 and Asp40–Gly46. Both of these regions form loops connecting a β-strand and α-helix. In the analysis at 1.5 Å resolution, it was reported that regions Ile12–Ser16 and Lys44–Thr45 show large differences between molecules *A* and *B*. In the present study, the crystal of BsL contains one molecule in the asymmetric unit. While some residues on the molecular surface are involved in intermolecular contacts within 4.0 Å to adjacent molecules, none of the residues around the active site take part in the contacts with the exception of His152–Val154, which is located in a loop region on the molecular surface. It was reported that molecule *A* in the previous analysis is free from molecular contacts in the crystal, which will explain the small r.m.s. distance (0.29 Å) between this molecule *A* and that in the present structure.

It was shown that BsL exhibits a high similarity to cutinase and acetylxylan esterase in structural architecture and in molecular size. The r.m.s. distances between C^{α} atoms of the present BsL and those of cutinase (Longhi *et al.*, 1997) and acetylxylan esterase (Ghosh *et al.*, 2001) are 1.5 and 1.9 Å, respectively, implying that the overall structures of BsL and cutinase or acetylxylan esterase are similar to each other. Structures of the active sites, especially the positional arrangements of the catalytic triad, are highly conserved.

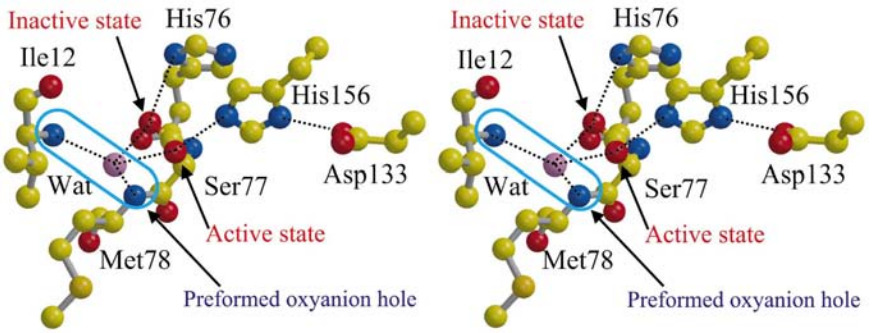

Figure 3
Stereoview of the catalytic triad (Ser77, Asp133 and His156). The side chains of Ser77 corresponding to the active and inactive states are labelled with arrows. The water molecule, which is incorporated in the oxyanion hole preformed by the main-chain N atoms Ile12 and Met78, is shown by a blue circle. Hydrogen bonds are represented by dotted lines.

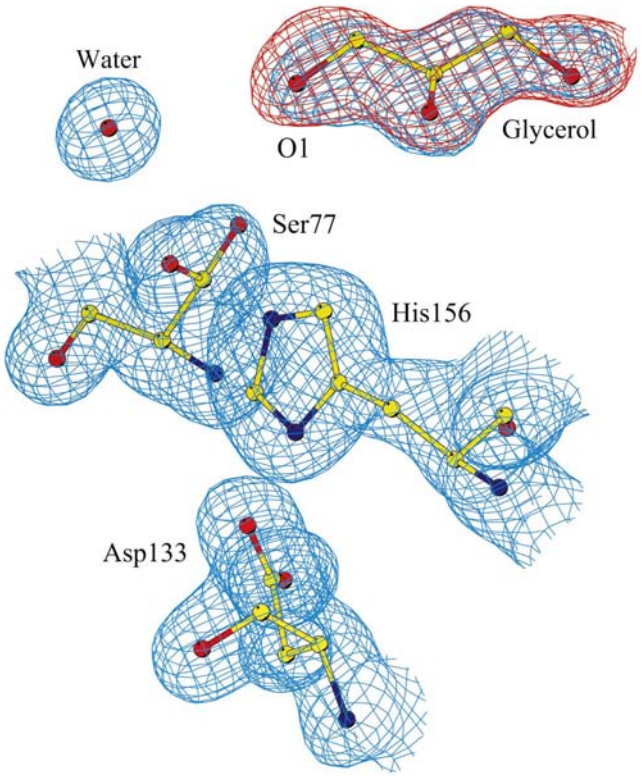

Figure 4
Omit map for the glycerol molecule at the active site. σ_A-weighted $2F_o - F_c$ and $F_o - F_c$ maps are drawn in blue and red, respectively. Each map is contoured at 2σ. One hydroxyl O atom of the glycerol is labelled O1.

The r.m.s distances between all non-H atoms of three residues are 0.12 Å for cutinase and 0.21 Å for acetylxylan esterase. Although in this superposition there are slight differences in orientations of the side chains of the catalytic serines and the imidazole rings of the catalytic histidines, the hydrogen-bond networks among the member of the catalytic triad are still conserved.

3.2. Alternate conformations of the side chain of the catalytic Ser77

For Ser77, one of the residues of the catalytic triad, alternate conformations of the side chain are identified. Fig. 2 shows two conformations of Ser77 and difference density maps which are calculated by omitting each O^{γ} atom of Ser77. The torsion angles χ_1 of the two conformations are −157 and 52°, respectively. Fig. 3 shows the networks of hydrogen bonds in the active site. In one conformation the O^{γ} atom of Ser77 makes a hydrogen bond to the N^{ε} atom of the catalytic His156. The side chain of His156 forms a further hydrogen bond to Asp133, a member of the catalytic triad. This conformation is therefore thought to correspond to an active state of BsL. On the other hand, the second conformer rotates the O^{γ} atom by about 150° from the active state and the O^{γ} atom is located at a distance of 3.3 Å from the N^{ε} atom of His76, which is not directly involved in the lipolytic reaction. This conformer therefore represents an inactive state. Although the occupancy of each conformer has not been refined, the occupancy of the active state seems to be slightly higher than that of the inactive state from examination of the electron density. The observation of two conformations of Ser77 suggests that BsL adopts a flip-flop movement at this residue, which corresponds to the active and inactive states.

In the structures of both cutinase and acetylxylan esterase, alternate conformers of the side chains of the catalytic serine residues (Ser120 for cutinase and Ser90 for acetylxylan esterase) are also observed. The resolutions of these structures are 1.0 and 0.9 Å, respectively. No alternate conformers in Ser77 are reported in the structure of BsL determined at 1.5 Å resolution, although the overall structure is similar to cutinase and acetylxylan esterase. The present structure determined at 1.3 Å resolution unambiguously reveals the existence of the conformers. It is supposed that the higher resolution in the present study allows us to distinguish the two conformers. Over 50 α/β-hydrolase folds have been reported in lipases and esterases. In these structural analyses, however, only cutinase and acetylxylan esterase have alternate conformations for their catalytic serines. The structural determinations of these two have been performed at extremely high resolution, while the resolutions of the others range from about 1.5 to 3.0 Å. Conformational variety at the active site of the enzyme is thought to be necessary for the enzymatic activity as it must be essential for the processes of substrate binding and product release. The present structure of BsL supports the existence of alternate conformations of the catalytic serine in its substrate-free state. The mobility of the side chain of Ser77 might be an important factor that determines the catalytic activity of this enzyme as it could affect the energy barrier between the active

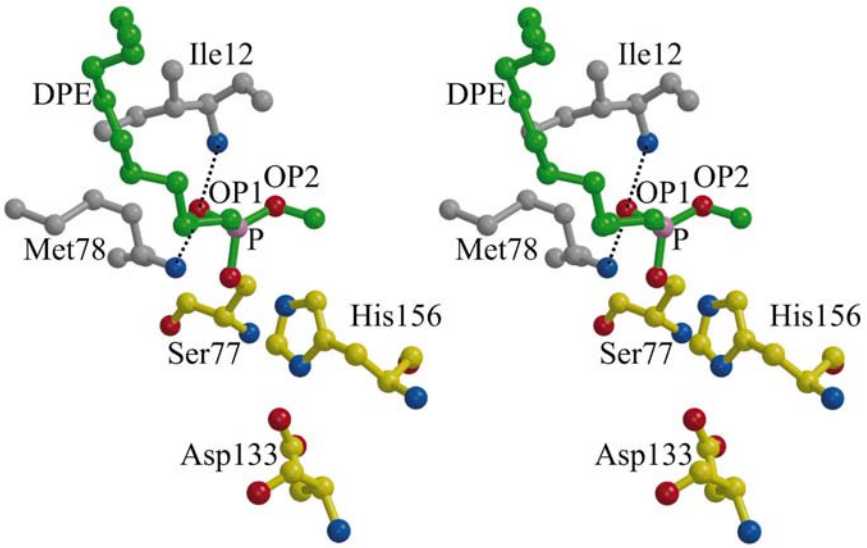

Figure 5
Structural model of BsL complexed with DPE calculated by superimposing the DPE–cutinase complex on that of BsL. The residues of the catalytic triad are shown as yellow bonds. Ile12 and Met78, which form the oxyanion hole, are shown as grey bonds. DPE is represented in green. Two phosphoric ester O atoms are labelled OP1 and OP2. OP1 is incorporated in the oxyanion hole which the water molecule occupies in the present structure.

and inactive states. If this hypothesis is true, it might be possible to improve the catalytic activity by site-directed mutagenesis, thus altering the hydrogen-bond network around the catalytic serine residue so that the mobility of this residue is increased.

3.3. Model of substrate-binding state

It has been reported that the intermediate of the catalytic reaction is stabilized by an oxyanion hole formed by two residues near the active site through hydrogen bonds between amide N atoms of the main chain and the O atom of the tetrahedral intermediate (Jaeger *et al.*, 1994). In BsL, Ile12 and Met78 are likely to form the oxyanion hole. A water molecule makes hydrogen bonds to both amide N atoms of Ile12 and Met78 (Fig. 3). In the substrate-free state of this enzyme, this water molecule is incorporated in the preformed oxyanion hole.

There is a glycerol molecule in the active site as shown in Fig. 4. The O1 atom of this glycerol is located within hydrogen-bonding distance of Ser77 O^{γ} in the inactive state. Moreover, several hydrophobic contacts are also observed between BsL and the glycerol. This glycerol appears to be specifically located at the active site. This glycerol therefore probably occupies the binding site of a free glycerol that is produced by the enzymatic reaction, although glycerol is only added to the crystallization solution as a cryoprotectant.

Of BsL, cutinase and acetylxylan esterase, only cutinase has been analyzed in complexes formed with four kinds of inhibitors. In order to gain insight into the catalytic mechanism of BsL, the structure of cutinase complexed with *n*-undecyl-*O*-methyl-chlorophosphonate ester (DPE; PDB code 1xzm) was superimposed on that of BsL to obtain a model of BsL complexed with DPE as shown in Fig. 5. It was found that the structure of the catalytic triad of cutinase superimposed well on that of BsL and that the resultant coordinates of DPE could smoothly be fitted onto BsL. This possible model of the BsL complex has no obstruction in terms of the DPE binding; the distance between Ser77 O^{γ} in the active state and the phosphoric ester P atom of DPE is 1.7 Å, which is close enough to form a covalent bond. It should be noted that the OP1 atom of DPE, a phosphoric ester O atom, is in the same position as the water molecule (Wat in Fig. 3) in the substrate-free state determined in the present study. This water molecule makes hydrogen bonds to both amide N atoms of Ile12 and Met78, which form the oxyanion hole. The OP1 atom of DPE corresponds to the O atom of the ester bond of acylglycerol, an original substrate of lipase. The previous study (van Pouderoyen *et al.*, 2001) proposed a model structure comprising the C8 inhibitor located in the active site of BsL on the basis of their 1.5 Å structure. Although the orientation of the fatty-acid group of the present DPE-binding model differs from that of the C8 inhibitor model, it appears that the positions of the P and O atoms of the phosphoric ester are almost the same. Although it is not clear whether DPE can act as an inhibitor for BsL, this model of the BsL–DPE complex suggests possible interactions between BsL and the inhibitor.

4. Conclusions

The structure of BsL determined in the present study at 1.3 Å resolution allows us to reveal the conformational variation of the side chain of the catalytic serine residue. In addition to alternate conformations of the catalytic serine found in cutinase and acetylxylan esterase, this structure suggests that all other enzymes containing an α/β-hydrolase fold and lacking the lid helices would have alternate conformations of their catalytic serine residues. Such structural information about the flip-flop movement of the side chain of the catalytic serine might be essential not only for understanding the mechanism of the catalytic reaction but also for the rational design of activity-improved mutants of this type of enzyme.

The experiments using synchrotron radiation were performed under the approval of the Photon Factory Advisory Committee, High Energy Accelerator Research Organization, Japan. We thank Drs N. Sakabe, N. Matsugaki and N. Igarashi of the Photon Factory for their kind help with data collection. This work was supported in part by a Grant-in-Aid for Scientific Research on Priority Areas (No.11169241) from the

Ministry of Education, Science, Sports and Culture, Japan to MS.

References

Brünger, A. T. (1992). *Nature (London)*, **355**, 472–475.

Brünger, A. T., Adams, P. D., Clore, G. M., DeLano, W. L., Gros, P., Grosse-Kunstleve, R. W., Jiang, J.-S., Kuszewski, J., Nilges, M., Pannu, N. S., Read, R. J., Rice, L. M., Simonson, T. & Warren, G. L. (1998). *Acta Cryst.* D**54**, 905–921.

Brzozowski, A. M., Derewenda, U., Derewenda, Z. S., Dodson, G. G., Lawson, D. M., Turkenburg, J. P., Bjorkling, F., Huge-Jensen, B., Patkar, S. A. & Thim, L. (1991). *Nature (London)*, **351**, 491–494.

Collaborative Computational Project, Number 4 (1994). *Acta Cryst.* D**50**, 760–763.

Dartois, V., Baulard, A., Schanck, K. & Colson, C. (1992). *Biochim. Biophys. Acta*, **1131**, 253–260.

Derewenda, U., Brzozowski, A. M., Lawson, D. M. & Derewenda, Z. S. (1992). *Biochemistry*, **31**, 1532–1541.

Derewenda, Z. S. (1994). *Adv. Protein. Chem.* **45**, 1–52.

Esnouf, R. M. (1997). *J. Mol. Graph.* **15**, 132–134.

Ghosh, D., Sawicki, M., Lala, P., Erman, M., Pangborn, W., Eyzaguirre, J., Gutiérrez, R., Jörnvall, H. & Thiel, D. J. (2001). *J. Biol. Chem.* **276**, 11159–11166.

Jaeger, K.-E., Ransac, S., Dijkstra, B. W., Colson, C., van Heuvel, M. & Misset, O. (1994). *FEMS Microbiol. Rev.* **15**, 29–63.

Jancarik, J. & Kim, S.-H. (1991). *J. Appl. Cryst.* **24**, 409–411.

Jones, T. A., Zou, J.-Y., Cowan, S. W. & Kjeldgaard, M. (1991). *Acta Cryst.* A**47**, 110–119.

Kabsch, W. & Sander, C. (1983). *Biopolymers*, **22**, 2577–2637.

Kraulis, P. J. (1991). *J. Appl. Cryst.* **24**, 946–950.

Lamzin, V. S. & Wilson, K. S. (1993). *Acta Cryst.* D**49**, 129–147.

Laskowski, R. A., MacArthur, M. W., Moss, D. S. & Thornton, J. M. (1993). *J. Appl. Cryst.* **26**, 283–291.

Lesuisse, E., Schanck, K. & Colson, C. (1993). *Eur. J. Biochem.* **216**, 155–160.

Longhi, S., Czjzek, M., Lamzin, V., Nicolas, A. & Cambillau, C. (1997). *J. Mol. Biol.* **268**, 779–799.

McPherson, A. (1990). *Eur. J. Biochem.* **189**, 1–23.

Matthews, B. W. (1968). *J. Mol. Biol.* **33**, 491–497.

Merritt, E. A. & Bacon, D. J. (1997). *Methods. Enzymol.* **277**, 505–524.

Misset, O., Gerritse, G., Jaeger, K.-E., Winkler, U., Colson, C., Schanck, K., Lesuisse, E., Dartois, V., Blaauw, M., Ransac, S. & Dijkstra, B. W. (1994). *Protein Eng.* **7**, 523–529.

Mustranta, A., Forssell, P. & Poutanen, K. (1993). *Enzyme Microb. Technol.* **15**, 133–139.

Ollis, D. L., Cheah, E., Cygler, M., Dijkstra, B., Frolow, F., Franken S. M., Harel, M., Remington, S. J., Silman, I., Schrag, J., Sussman, J. L., Verschueren, K. H. G. & Goldman, A. (1992). *Protein Eng.* **5**, 197–211.

Perrakis, A., Sixma, T. K., Wilson, K. S. & Lamzin, V. S. (1997). *Acta Cryst.* D**53**, 448–455.

Pouderoyen, G. van, Eggert, T., Jaeger, K.-E. & Dijkstra, B. W. (2001). *J. Mol. Biol.* **309**, 215–226.

Powell, H. R. (1999). *Acta Cryst.* D**55**, 1690–1695.

Ramakrishnan, C. & Ramachandran, G. N. (1965). *Biophys. J.* **5**, 909–933.

Read, R. J. (1986). *Acta Cryst.* A**42**, 140–149.

Rossmann, M. G. & van Beek, C. G. (1999). *Acta Cryst.* D**55**, 1631–1640.

Sambrook, J., Fritsch, E. F. & Maniatis, T. (1989). *Molecular Cloning: a Laboratory Manual*, 2nd ed, edited by N. Ford, C. Nolan, M. Ferguson & M. Ockler. New York: Cold Spring Harbor Laboratory Press.

Sarda, L. & Desnuelle, P. (1958). *Biochim. Biophys. Acta*, **30**, 513–521.

Sheldrick, G. M. & Schneider, T. R. (1997). *Methods Enzymol.* **277**, 319–343.

Terwilliger, T. C. (2000). *Acta Cryst.* D**56**, 965–972.

Terwilliger, T. C. & Berendzen, J. (1999). *Acta Cryst.* D**55**, 849–861.